www.ietdl.org

Published in IET Image Processing
Received on 2nd July 2013
Revised on 18th October 2013
Accepted on 26th November 2013
doi: 10.1049/iet-ipr.2013.0471

ISSN 1751-9659

# New approach for the detection of noise-distorted signals based on the method of S-preparation

*Leonid I. Timchenko[1], Yuriy F. Kutayev[2], Serhiy V. Cheporniuk[3], Nataliya I. Kokriatskaya[1], Andriy A. Yarovyy[4], Alyona E. Denysova[1]*

*[1]Department of the Telecommunication Technologies and Automation, State Economic Technological University of Transport, Kyiv, Ukraine*
*[2]Department of KIA Systems JSC Design Bureau, Moscow, Russian Federation*
*[3]Department of Control System Design, LLC "KSK-Automation", Kyiv, Ukraine*
*[4]Department of Computer Science, Vinnytsia National Technical University, Vinnytsia, Ukraine*
*E-mail: timchen@list.ru*

**Abstract:** A classification of correlation algorithms is provided. A method of S-preparation is discussed, which, due to the preliminary conveyor formation of correlated image convolution sums, is characterised by high noise immunity and adaptivity to uncertainty and variability of the signal clutter situation.

## 1 Introduction

Creation of automated correlational coordinates meters, where a functional for the connection between a current and a reference images is calculated and coordinates of this functional's extremum are determined, gains a special importance today [1–5].

The advantages of correlation-extremal coordinates meters (CECM) include a possibility to work in the uncertain signal clutter situation, a large current image frame and resistance to de-correlating factors (sensitivity inhomogeneity, noise, geometrical distortion of the video sensor, errors of analogue-to-digital transformation, etc.).

The S-preparation method, suggested in this paper, and a device that realises it, calculate contour preparations (labels) based on the initial image counting and a cross-correlation function of resulting labels [2, 6].

Modern radio-technical systems designed for different purposes need to work under difficult signal clutter situations. Development of the communication, radiolocation and other systems increasingly faces a problem of detecting noise-distorted signals, when their characteristics are subject to changes or not known in advance. In such systems, signals, called images, are functions of two space coordinates and time. A physical meaning of the correlational processing in such cases is in matching images.

The classification of correlational algorithms, their advantages and drawbacks are shown in Table 1 [3, 4, 7–18]. There are several levels of image predictability, with their corresponding correlation algorithms. A given level of image predictability is suited by an algorithm of the same or lower level.

At the first predictability level, the image intensities can be predicted accurately in relation to the absolute level; here, difference correlational algorithms determine a minimum of the square of difference, and a minimal absolute difference may be used. The second predictability level helps in assessing a difference in intensities in relation to an absolute level with a possible random shift and uses different correlational algorithms normalised to the average level. The third predictability level would evaluate relative intensities (i.e. element $i$ is brighter than element $j$), but can hardly predict a scale. At this level, a normalised classic correlational algorithm and an algorithm of the amplitude rating are used. At the fourth predictability level, areas with different intensities may be located, but relative intensities are unpredictable (intensity inversion is possible), and unpredictable elements are possible, including perspective distortions. At this level, correlational algorithms with preliminary current images processing (isolation of contours or other predictable characteristics) are used. Therefore, the higher the level of predictability, the more determined is the image and simpler is the algorithm structure. Let us briefly characterise the algorithms of correlational processing.

A classic algorithm of correlational processing calculates the cross-correlation function or the integral convolution with further retrieval of this function's maximum. However, the classic algorithm is highly intensive computationally, as calculation of the cross-correlation function is conducted under all possible shifts of the processed images. If the images have sizes of $M \times M$ and $N \times N$ pixels, then a number of points for which the correlation function is calculated is $(N - M + 1)^2$. Usually, it is a significant number.

The difference correlation algorithms are based on the element-by-element calculation of the image intensity difference.

From the perspective of the computational costs, difference algorithms are preferable to the classic algorithm, because they do not contain an operation of multiplication. A class of difference correlation algorithms includes also an

**Table 1** Classification of correlation algorithms

| Method of correlation processing<br>1 | Approach to image processing<br>2 | Advantages<br>3 | Drawbacks<br>4 |
|---|---|---|---|
| Optimal space filtration [7] | Images are filtered to optimise matching. Optimal filters are constructed using typical images | Increased ratio of the main peak of the correlation function to the side peaks. Homogeneity of side lobes. Possibility of the analytical description | Based on the knowledge of the grey level of the image. Construction of the filter requires evaluation of the noise statistics |
| Background correlation [8, 9] | Area correlation with the use of the inverse Fourier transformation of the mutual energy spectrum of the phase | Sharp correlation peaks. Realisation efficiency. Resistance to narrow-band noise | Requires prediction of the grey level of images. Requires a broadband image subject |
| Binary correlation [10] | Images are being preliminary binarised | Efficient digital realization. Reduced sensitivity to errors in predicting the grey level | Requires prediction of the grey level of images. Information value of images decreases as a result of transfer to binary images |
| Correlation of transformation coefficients [11] | Processing with the algorithm of the minimal absolute difference of Hadamard coefficients of the reference and current images | Increased peak sharpness. Decreased sensitivity to noises. Developed with a preliminary processor of geometric images | Requires prediction of the grey level of images. Increased computational intensity |
| Optical matched filter [12] | Analogue matched filter with the use of coherent processing of light | Practically instant correction. Exceptionally big memory capacity. Parallel processing of several reference images | Based on prediction of the grey level. Processing flexibility is constrained by hardware implementation |
| Three-dimensional correlation [4, 13] | A three-dimensional model of the target and data of the active range finder are matched | Prediction of the grey level is not required. All possible lateral angles of approach can be taken into account. Resistant to deliberate changes in the target features | Requires a range finder. Significant computational intensity |
| Matching of relative information vectors (RIV characterises each indicator on the basis of neighbouring indicators) [5] | Matching is based on the maximisation of the number of respective RIVs | Prediction of the grey level is not required. Includes three-dimensional object. Insensitive to contrast inversion. Maximal requirements to the memory | Feature extraction. Sensitive to noise. Analytical description of characteristics is complicated |
| Matching of structural models [14] | Structural models of features (lines, segments, tops, spots) are matched | Prediction of the grey level is not required. Insensitive to contrast inversion. Minimal requirements to the memory | Feature extraction. Sensitive to noise. Analytical description of characteristics is complicated |
| Contour preparation [15] | Three-level binarisation with the adaptive threshold limitation is conducted | Simplicity of implementation. Resistant to noise signals | Information capacity of images decreases due to transfer to binarised images |

algorithm of consequential determination of the image likeness. In regular difference algorithms, a measure of image likeness is calculated under all possible positions of the current image in relation to the reference image. However, obviously, precise calculations make sense only for a small number of points near the correlation function maximum. That is why in the algorithm of consequential determination of image likeness, a position with the smallest total error, for which a threshold value is set, is taken as a matching position. The algorithm of consequential determination of image likeness significantly decreases the amount of calculations.

A correlation algorithm of amplitude rating was developed for applications where a very large search space is being processed, and, consequently, which have high requirements to the computational efficiency. The correlation algorithm of amplitude rating is a family of correlation algorithms, whose level of complexity and computational efficiency can be optimised for certain parameters of particular systems. For instance, a binary amplitude-rating algorithm includes two stages. At the first stage, preliminary processing is conducted, when a smaller image is being coded into binary correlational matrixes. At the second stage, those binary matrices are consequentially correlated with a decreasing subset of the bigger-sized matrix. The stage of preliminary processes includes ranging the image elements in the order of decreasing intensity and assigning a binary rank to each element. If the image has $2^n$ resolution elements (pixels), then the element with the lowest intensity receives a rank consisting of $n$ zeros, and the element with the highest intensity receives a rank consisting of $n$ ones. Other elements are assigned ranks corresponding to a binary number of the element in the ordered list. Then elements are split into groups by intensity, until just one element remains in each group. Then correlational matrices are formed by mapping signs of binary ranks on the initial image, and correlational surfaces are calculated, with each following surface being a refining of the previous one. The correlational surface is calculated in the following way: for each position of the correlational matrix on the big image, a sum of elements in the points corresponding to zeros in the matrix is distracted from sums of elements corresponding to ones at the same point. After the last surface is calculated, a point with the maximum value is determined; this point is a matching point of images. The amount of computation for the amplitude rank algorithm


IET Image Process., 2014, Vol. 8, Iss. 11, pp. 627–638
doi: 10.1049/iet-ipr.2013.0471

(characterised by a number of operations of addition) is

$$A = B \times (M - m) \times (K - k) \times m \times k$$

where $B$ is a coefficient ($1 < B < 2$); $M$, $K$ are the sizes of the big image; $m$, $k$ are the sizes of the small image.

The amplitude rank algorithm is an analogue to the classic correlation algorithm, with both algorithm having practically the same characteristics of matching accuracy and probability.

The abovementioned algorithms are developed for correlational processing of images with a plane-parallel shift. That is why algorithms are sensitive to rotation of images, and as rotation angle increases, the efficiency of such algorithms drops significantly. However, an algorithm of correlational processing using sums of gradient vectors is invariant to rotation in the significant range of angle. At the first stage of this algorithm, gradients of the grey level for both images are calculated. At the second stage, a histogram of gradient vector sums is being formed for each image from gradient vectors falling into discrete intervals of angles. Then those functions are processed with a classic correlation algorithm, or using an algorithm of phase correlation [19]. The algorithm is based on the fact that if one image is rotated for a certain angle, the gradient vector calculated for respective elements of both images will turn for the same angle. However, the values of the average gradient are usually very close to zero, which makes this method critical towards errors introduced by changes in low space frequencies.

In 2000, fast correlation algorithms were developed, in particular, those based on the methods of contour preparation and S-preparation, which, due to the preliminary pipeline processing of convolution sums of the correlated images, are distinguished for high noise immunity and adaptability to uncertainty and unsteadiness of the signal clutter situation [16]. Recently, a topic on the image correlational analysis with various processing methods received further development [5, 20]. In particular, it is a method of S-preparation, which is the main theme of this paper.

## 2 Method of *S*-preparation

The method of *S*-preparation is a modified method of contour preparation [15, 21], where contour labels are formed from normalised convolutions of initial images, and the summation window, by which average sums of convolution are calculated, shifts within its initial position.

An idea to reduce the computational intensity by representing an image as an incomplete W-spectrum and to simplify when pre-processing correlated images by the adaptive method of generalised contour preparation is used here, as well.

Therefore, the idea of this method is to find an image fragment that includes the most informative (according to the varied criterion) fragment of the background, and to perform the correlation-extremal measuring of this fragment's inter-frame shift with further preparation of the measured shift to the unknown shift of the background; here, fragment sizes fall in between the size of the dynamic object and the extended background.

A method of comparing contour preparations with the summation window shift (method of S-preparation) is suggested for use in the CECM to determine the background shift contained in the current processed image.

An algorithm of the extended object localisation with the preliminary convolutional summing of the image is brought down to the following operations:

1. A field of frame of the two-dimensional image with size $n \times n$ pixels is split into $(n/m)^2$ fragments of $m \times m$ pixels, and convolutions by fragments (average sums of pixels by fragments) are accumulated:

$$\tilde{f}(k, l) = \frac{\sum_{j=l(n/m)}^{(l+1)(n/m)-1} \sum_{i=k(n/m)}^{(k+1)(n/m)-1} \tilde{f}(i, j)}{mm}$$

where $\tilde{f}(i, j)$ is a digital count (pixel) of the image with coordinates $i, j$; $(k, l)$ is a number of the image fragment: $k = \overline{0, (n, m) - 1}$; $l = \overline{0, (n, m) - 1}$.

2. The accumulated convolutes $\tilde{f}(k, l)$ of the current image are stored and used as convolutes $\bar{f}_g(k, l)$ of the delayed image in the next frame.

3. A fragment $(k_m, l_m)$ is selected, for which an absolute value of difference between current and delayed image convolutes is minimal

$$(k_m, l_m) = \min\left\{ |\bar{f}(k, l) - \bar{g}(k, l)|;\ k = \overline{0, \frac{n}{m} - 1};\ l = \overline{0, \frac{n}{m} - 1} \right\}$$

4. A local difference threshold $\delta_f$ is calculated necessary for contour labelling the selected fragment pixels through the pipeline accumulation of a sum $\bar{f}^{>}$ of counts of big convolutions and a sum $\bar{f}^{<}$ of smaller convolutions $\bar{f}(k, l)$.

5. By the fragment $(k_m, l_m)$

$$\delta_f = \frac{1}{2}\left(\bar{f}^{>} - \bar{f}^{<}\right)$$

6. An array of contour labels is being formed by means of pipeline accumulation of differences $S_f(i, j)$ on the surroundings of each pixel $\bar{f}(i, j)$

$$\left\{ q_f(i, j), \quad \text{where} \quad \cdot\, i = \overline{k\frac{n}{m}, (k+1)\frac{n}{m} - 1}; \right.$$

$$\left. j = \overline{l\frac{n}{m}, (l+1)\frac{n}{m} - 1} \right\}$$

$$S_f(i, j) = \frac{1}{2}\left[\left(\tilde{f}(i, j-1) + \tilde{f}(i-1, j)\right) - \left(\tilde{f}(i+1, j) + \tilde{f}(i, j+1)\right)\right]$$

$$q_f(i, j) \in \left\{ \overset{+}{q}_f(i, j), \quad \overset{0}{q}_f(i, j), \quad \overset{-}{q}_f(i, j) \right\}$$

As a result, positive $\overset{+}{q}_f(i, j)$, zero $\overset{0}{q}_f(i, j)$ and negative $\overset{-}{q}_f(i, j)$ labels of counts $S_f(i, j)$ are formed, where $\in$ is a


doi: 10.1049/iet-ipr.2013.0471

sign of belonging, and

$$S_f(i,j) = \begin{cases} \overset{+}{q}_f(i,j) = 1, & S_f(i,j) > \delta_f \\ \overset{0}{q}_f(i,j) = 0, & \left|S_f(i,j)\right| \le \delta_f \\ \overset{-}{q}_f(i,j) = -1, & S_f(i,j) < -\delta_f \end{cases}$$

7. An array of the current image contour labels $\left\{\overset{+}{q}_f(i,j),\ \overset{0}{q}_f(i,j),\ \overset{-}{q}_f(i,j)\right\}$ is stored and used as a delayed image in the next frame;

8. A local difference threshold of the delayed image $\delta_g$ is formed

$$\delta_g = \frac{1}{2}\left(\overline{g^{>}} - \overline{g^{<}}\right)$$

as well as contour labels

$$q_g(i,j) \in \left\{\overset{+}{q}_g(i,j),\ \overset{0}{q}_g(i,j),\ \overset{-}{q}_g(i,j)\right\}$$

9. The rank cross-correlation function (RCCF) $R(k_m, l_m)$ of the fragment $(k_m, l_m)$ is calculated.

10. Coordinates $(X_{f_{\max}}, Y_{f_{\max}})$ of the RCCF $R(k_m, l_m)$ maximum are calculated.

11. A shift of the current image background in relation to the delayed image background is found

$$\begin{cases} \Delta X = X_{f\max} - X_{\max} \\ \Delta Y = Y_{f\max} - Y_{\max} \end{cases}$$

A shift of the summing window that corresponds to the maximal count of the count array of the RCCF is the true shift of background in the current image in relation to the delayed one.

Two ways of contour label formation are useful: unary formation and sign formation.

The current image unary formation

$$q_f(i,j) \in \left\{\overset{+}{q}_f(i,j),\ \overset{0}{q}_f(i,j),\ \overset{-}{q}_f(i,j)\right\}$$

$$\overset{+}{q}_f(i,j) = \begin{cases} 1, & S_f(i,j) > \delta_f \\ 0, & S_f(i,j) \le \delta_f \end{cases}$$

$$\overset{0}{q}_f(i,j) = \begin{cases} 1, & \left|S_f(i,j)\right| \le \delta_f \\ 0, & \left|S_f(i,j)\right| > \delta_f \end{cases}$$

$$\overset{-}{q}_f(i,j) = \begin{cases} 1, & S_f(i,j) < -\delta_f \\ 0, & S_f(i,j) \ge -\delta_f \end{cases}$$

Therefore, in case of unary formation, the array $\{S_f(i,\ j)\}$ transforms into three arrays $\left\{\overset{+}{q}_f(i,j)\right\}$, $\left\{\overset{0}{q}_f(i,j)\right\}$ and $\left\{\overset{-}{q}_f(i,j)\right\}$.

The unary formation of the delayed image in relation to the threshold $\delta_g$ is performed in a similar way; as a result, three arrays are formed: $q_g(i,j) \in \left\{\overset{+}{q}_g(i,j),\ \overset{0}{q}_g(i,j),\ \overset{-}{q}_g(i,j)\right\}$.

The unary formation makes it possible to simplify computation of the rank CCF (RCCF) due to the substitution of the arithmetic multiplication operation with the logical multiplication (conjunction)

$$R_{fg}(\boldsymbol{\tau}) = \sum_{\{(i,j)\}} \overset{+}{q}_f\left(i-\tau_x,\ i-\tau_y\right) \wedge \overset{+}{q}_g(i,j) + \sum_{\{(i,j)\}} \overset{0}{q}_f\left(i-\tau_x,\ i-\tau_y\right) \wedge \overset{0}{q}_g(i,j) + \sum_{\{(i,j)\}} \overset{-}{q}_f\left(i-\tau_x,\ i-\tau_y\right) \wedge \overset{-}{q}_g(i,j)$$

where ^ is a sign of logical multiplication (conjunction); $\boldsymbol{\tau}$ is a shift vector.

Such substitution allows to reach maximal performance in calculating the RCCF while using a parallel optical electronic adder.

In addition, in case of unary formation, the maximal possible value of the CCF is equal to the maximal value of the rank autocorrelation function (RACF), which is equal to the number of counts $N_r$ of each of compared rank contour preparations of the current and delayed images, that is, $N_{f_0 r} = N_{g_0 r} = N_{r_0}$.

Therefore, dividing values of RCCF counts by the known number $N_r$ leads to their normalisation and, respectively, to transformation of the field of RCCF counts into the field of correlation coefficients of rank contour preparations of the current and delayed images. Number $N_r$ is known a priori; thereby, division of RCCF count field values by $N_r$ is not required.

Therefore, calculation of a classic correlation coefficient of rank contour labels of the current and delayed images (that requires calculating their RCCF, finding a label with the maximal RCCF value, calculating a maximal value for the RACF of the delayed image and dividing a square root of the maximal RCCF value by maximal RACF value with further estimation of the maximal value of the correlation coefficient) is substituted with calculating the RCCF, finding a count with maximal RCCF and its comparison with the number $N_r(1-\delta_k)$, where $1-\delta_k$ is a preset threshold, and $0<\delta_k<1$. For instance, if $1-\delta_k=0,\ 9$, a maximal number of matching values of the compared rank contour preparations of the current and delayed image for each shift vector of the current image in relation to the delayed image should be at least $0,\ 9N_r$.

The sign formation of the current image

$$q_f(i,j) \in \left\{\overset{+}{q}_f(i,j),\ \overset{0}{q}_f(i,j),\ \overset{-}{q}_f(i,j)\right\}$$

$$q_f(i,j) \in \left\{\overset{+}{q}_f(i,j),\ \overset{0}{q}_f(i,j),\ \overset{-}{q}_f(i,j)\right\}$$

$$q_f(i,j) = \begin{cases} \overset{+}{q}_f(i,j) = 1 & S_f(i,j) > \delta_f \\ \overset{0}{q}_f(i,j) = 0 & \left|S_f(i,j)\right| \le \delta_f \\ \overset{-}{q}_f(i,j) = -1 & S_f(i,j) < -\delta_f \end{cases}$$



doi: 10.1049/iet-ipr.2013.0471

In case of sign preparation, two bits are required for presenting a label of prepared pixel of the current image.

The sign formation of the prepared pixel of the current image in relation to the threshold $\delta_g$ is performed similarly.

In case of sign preparation, all calculations should be conducted, which are required to find a classic correlation coefficient of rank contour labels of the current and delayed images. Simplified computation and enhanced performance are achieved through two-digit operands in the arithmetic multiplication operation in calculating the RCCF and RACF, respectively; and a decrease in the range of maximal values of the RCCF and the RACF is achieved, and so on.

A modified method of S-preparation (a method of S-preparation with correction), consisting of forming convolutes of image counts under various shifts of the summing window, formation of this basis convolutes of contour labels using an optimal local difference threshold and comparing the obtained preparations of the current image with those of the delayed image under a zero shift of the summing window. This method allows to find coordinates of the true shift of the image background with accuracy of up to one pixel when a true RCCF peak exceeds a maximal false peak for most background types of the image, except for some cases of backgrounds with regular structure (e.g. sinusoidal).

The influence of noise on one-dimensional signals of the object and the background was modelled in the research. Two main kinds of noise were considered: with the uniform and the normal (Gaussian) distribution of the probability density. Amplitude of the noise count $r_i$ with the uniform distribution may be determined as

$$r_i = \frac{R}{100} \times \text{RND} \times N_{\max}$$

where $R$ is the degree of the noise pollution of the array of signal counts (%); $N_{\max}$ is the maximal amplitude of signal counts; RND is a random number within the range of 0–1, formed by the uniform random function.

The noise pollution of the signal was conducted by adding a signal count to the respective noise count.

With the normal distribution of the probability density $P(x)$, the formula is true

$$P(x) = \frac{1}{\sqrt{2 \times \pi \times \sigma}} \times e^{-((x-a)^2/4\pi)}$$

where $x$ is an amplitude of a random noise count; $a$ is a mathematical expectation of noise counts; $\sigma$ is a root-mean-square deviation of noise counts.

The '3$\sigma$ rule' is true, that is

$$\sigma = \frac{G \times N_{\max}}{100 \times 3}$$

where $G$ is a degree of noise pollution of the array of signal counts with the Gaussian noise (%).

For the noise counts with the amplitude $x_i = 0, 1, 2, 3, \ldots$ and mathematic expectation equal to zero, the probabilities are found as

$$P(x) = \frac{1}{\sqrt{2 \times \pi \times \sigma}} \times \int_{x_i}^{x_i+1} e^{-(x^2/4\pi)}\, \mathrm{d}x$$

and an array of noise counts is formed, where a number of noise counts with the amplitude $x_i$ corresponds to the calculated probability $P(x_i)$, that is

$$P(x_i) \simeq \frac{N(x_i)}{N_{\text{total}}}$$

where $N(x_i)$ is the number of noise counts with amplitude $x_i$; $N_{\text{total}}$ is the total number of noise counts of the array.

A signal/noise ratio was determined as a ratio of true/false peaks of count arrays of the RCCF. The value of the true peak $R(x_u)$ of RCCF was determined by the a priori set true shift of background $x_u$. A value of the maximal false peak is determined in the following way.

From the array of RCCF counts, those counts are excluded, for which

$$R(x_u + 1 + i) = \begin{cases} 0 & \text{if } R(x_u - 1) - R(x_u - 1 - i) > 0 \\ R(x_u + 1 + i) & \text{otherwise} \end{cases} \quad \text{for } i = \overline{0, x_{\max} - x_u}$$

$$R(x_u - 1 - i) = \begin{cases} 0 & \text{if } R(x_u - 1) - R(x_u - 1 - i) > 0 \\ R(x_u - 1 - i) & \text{otherwise} \end{cases} \quad \text{for } i = \overline{0, x_u - 1}$$

In the remaining counts, a count is found with the maximal amplitude $R(x_u)$. It is the maximal false peak.

Therefore, the method of S-preparation allows to find a value of the background shift for the delayed and current image.

In the CECM, which work with count arrays of large images (512 × 512), we suggest using a two-stage procedure for determining the value of background shift:

- Split initial arrays of image pixels into fragments and select a fragment by the criterion of the minimal background distortion;
- Process the selected current and delayed image fragments with the method of S-preparation.

We suggest the method of S-preparation to be used in the so-called 'crude' channel of the two-channel CECM (its structure chart is presented in Fig. 1).

The discussed CECM works in the following way: an input image is being transformed with the video sensor 1 and analogue-to-digital conversion unit 2 into a digital form and then, through the preliminary processing unit 3, and the frame delay unit 4 is sent to the CECM 'crude' channel 5, where the method of S-transformation is being realised, that allows to find coordinates of the shift background contained in the image for large images (≃512 × 512). The 'crude' channel 5 processes digital counts of the current and delayed images. The coordinates of background shift from the output of the 'crude' channel 5 are sent to the system controller 7 that forms a command for the shift of the current image frame in the preliminary processing unit 3, opposite to the shift calculated in the 'crude' channel 5. After that, reduction of frames of the delayed image and shifted current image is conducted in unit 3, resulting in the formation of the image frame that contains the object at zero level. A fragment of this image that contains the object goes to the CECM 'precise' channel 6, where true coordinates of the object shift are determined.


doi: 10.1049/iet-ipr.2013.0471

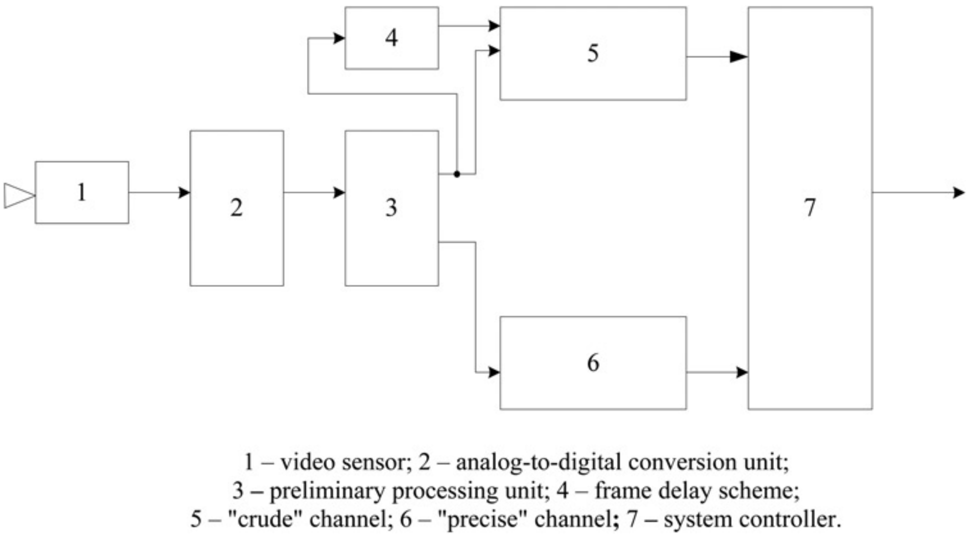


**Fig. 1** *Block chart of the two-channel correlation-extremal coordinates meter*

To characterise a method realised in the 'crude' channel 5, the term 'S-preparation' was introduced. Although it is based on the method of contour preparation, an operation of preparation is performed not on counts of initial images, but on so-called convolutions, or sums of counts within the summing window formed by splitting a count array of initial images into fragments, or summing windows. Such convolutions are calculated for different shifts of the summing window, and according to the method of contour preparation, counts of RCCF are found that correspond to summing window shifts, and a shift degree is then determined by extremums.

## 3 Experimental research and software modelling results

Methods of contour preparation and two suggested methods of S-preparation were compared by a criterion of the true/false peaks ratio for arrays of random and sinusoidal counts of background under various degrees of noise pollution of arrays with uniform and Gaussian noise and various lengths of rank vector. The comparison results are presented in Tables 2–5 and Figs. 2–5.

A count in the RCCF count array that corresponds to a priory set true background shift was taken as a true peak, and a maximal count of the remaining RCCF counts was taken as a false peak. The background shift in the current image and its noise pollution result in changes in values of fragment convolutions, and in a number and relative position of positive, negative and zero labels. As a result, coordinates of the maximal RCCF peak may not correspond to the true (a priory set) background shift. If in this case a value of this (false) peak is smaller than the RCCF count value corresponding to the true background shift, a ratio of the true peak to the false one will be <1. Let us explain the above with the following example:

Undistorted background preparation:
[+ + + 0 0 0 – – –] 0 +
The background preparation distorted by noise:
[+ 0 0 0 0 – – – –] 0 +
A shifted undistorted background preparation ($\tau = 1$):
[+ + + 0 0 0 – – –] 0 +

**Table 2** Comparison of preparation methods for the true/false peak ratio under different grades of uniform noise pollution of random counts and different lengths of the rank vector

| Length of the rank vector | Processing method | Noise pollution, % | | | | |
|---|---|---|---|---|---|---|
| | | 0 | 5 | 10 | 15 | 20 |
| $r = 1$ | Method of contour preparation [15, 17] – the closest method | 2.07 | 1.92 | 1.93 | 1.91 | 1.66 |
| | suggested method of S-preparation | 1.75 | 1.0 | 1.08 | 1.85 | 0.75 |
| | Suggested method of S-preparation with correction | 2.8 | 1.25 | 1.5 | 1.0 | 0.73 |
| $r = 2$ | Method of contour preparation [15, 17] – the closest method | 2.24 | 2.11 | 1.96 | 1.6 | 1.57 |
| | suggested method of S-preparation | 0.93 | 0.92 | 1.0 | 1.0 | 0.91 |
| | Suggested method of S-preparation with correction | 1.18 | 0.91 | 1.0 | 1.0 | 1.13 |
| $r = 3$ | Method of contour preparation [15, 17] – the closest method | 2.39 | 2.09 | 2.15 | 1.63 | 1.58 |
| | Suggested method of S-preparation | 1.33 | 1.0 | 1.1 | 1.13 | 0.73 |
| | Suggested method of S-preparation with correction | 1.33 | 1.11 | 1.38 | 1.14 | 0.7 |

A shifted distorted background fragment ($\tau = 1$):
[+ 0 0 + – – + – –] – 0
A shifted distorted background fragment ($\tau = 2$):
[– – 0 0 – + – 0 0] – –
A value of the RCCF counts of background preparations 2 and 4:
$\tau = 1$ $R(1) = 6$
A value of the RCCF counts of background preparations 2 and 5:
$\tau = 2$ $R(2) = 4 < R(1) = 6$,

which was to be shown.


*IET Image Process.*, 2014, Vol. 8, Iss. 11, pp. 627–638
doi: 10.1049/iet-ipr.2013.0471

**Table 3** Comparison of preparation methods for the true/false peak ratio under different grades of uniform noise pollution of sinusoidal counts and different lengths of the rank vector

| Length of the rank vector | Processing method | Noise pollution, % | | | | |
|---|---|---|---|---|---|---|
| | | 0 | 5 | 10 | 15 | 20 |
| $r=1$ | Method of contour preparation [15, 17] – the closest method | 1.35 | 0.86 | 1.0 | 0.82 | 0.71 |
| | Suggested method of S-preparation | 1.0 | 1.0 | 1.0 | 0.92 | 0.86 |
| | Suggested method of S-preparation with correction | 1.0 | 1.0 | 1.0 | 0.89 | 0.5 |
| $r=2$ | Method of contour preparation [15, 17] – the closest method | 8.79 | 1.05 | 0.85 | 0.91 | 0.81 |
| | Suggested method of S-preparation | 1.0 | 0.62 | 0.91 | 0.69 | 0.91 |
| | Suggested method of S-preparation with correction | 1.0 | 0.62 | 0.82 | 0.71 | 1.0 |
| $r=3$ | Method of contour preparation [15, 17] – the closest method | 15.25 | 0.86 | 0.89 | 0.92 | 0.76 |
| | Suggested method of S-preparation | 1.0 | 1.0 | 1.0 | 1.0 | 0.85 |
| | Suggested method of S-preparation with correction | 1.0 | 1.0 | 0.91 | 0.78 | 0.7 |

**Table 4** Comparison of preparation methods for the true/false peak ratio under different grades of Gaussian noise pollution of random counts and different lengths of the rank vector

| Length of the rank vector | Processing method | Noise pollution, % | | | | |
|---|---|---|---|---|---|---|
| | | 0 | 5 | 10 | 15 | 20 |
| $r=1$ | Method of contour preparation [15, 17] – the closest method | 2.07 | 2.07 | 1.9 | 1.9 | 1.9 |
| | Suggested method of S-preparation | 1.75 | 1.56 | 1.0 | 1.0 | 1.0 |
| | Suggested method of S-preparation with correction | 2.8 | 1.75 | 3.5 | 1.56 | 1.11 |
| $r=2$ | Method of contour preparation [15, 17] – the closest method | 2.24 | 2.02 | 1.98 | 2.02 | 1.89 |
| | Suggested method of S-preparation | 0.93 | 0.92 | 1.0 | 1.17 | 0.92 |
| | Suggested method of S-preparation with correction | 1.18 | 1.09 | 1.2 | 1.17 | 1.0 |
| $r=3$ | Method of contour preparation [15, 17] – the closest method | 2.39 | 2.42 | 2.09 | 1.93 | 1.9 |
| | Suggested method of S-preparation | 1.3 | 1.2 | 0.82 | 1.11 | 1.0 |
| | Suggested method of S-preparation with correction | 1.3 | 1.2 | 0.82 | 1.11 | 1.0 |

The advantages of the method of background shift assessment using comparison of contour labels of normalised convolutions with summing window shift include:

**Table 5** Comparison of preparation methods for the true/false peak ratio under different grades of Gaussian noise pollution of sinusoidal counts and different lengths of the rank vector

| Length of the rank vector | Processing method | Noise pollution, % | | | | |
|---|---|---|---|---|---|---|
| | | 0 | 5 | 10 | 15 | 20 |
| $r=1$ | Method of contour preparation [15, 17] – the closest method | 1.35 | 1.23 | 0.89 | 0.80 | 1.03 |
| | Suggested method of S-preparation | 1.0 | 1.0 | 1.0 | 1.0 | 1.0 |
| | Suggested method of S-preparation with correction | 1.0 | 1.0 | 1.0 | 1.0 | 1.0 |
| $r=2$ | Method of contour preparation [15, 17] – the closest method | 8.79 | 1.32 | 0.94 | 0.94 | 0.8 |
| | Suggested method of S-preparation | 1.0 | 1.0 | 0.82 | 1.2 | 0.57 |
| | Suggested method of S-preparation with correction | 1.0 | 1.0 | 0.82 | 1.22 | 0.57 |
| $r=3$ | Method of contour preparation [15, 17] – the closest method | 15.25 | 8.15 | 0.97 | 0.97 | 0.92 |
| | Suggested method of S-preparation | 1.0 | 1.0 | 1.0 | 1.0 | 1.0 |
| | Suggested method of S-preparation with correction | 1.0 | 1.0 | 1.0 | 1.0 | 1.0 |

1. the noise is averaged when computing normalised convolutions;
2. Chebyshev measure is used in selecting a fragment (p. 9, paragraph c);
3. in case of the unary formation of contour labels, the shift vector of fragment background is found by computing a correlation coefficient (p. 9, paragraphs *h*, *i* and *j*).

A combination of those advantages secures enhanced noise immunity and accuracy of this method, while at the same time maximally simplifies the calculations.

The ratio of true/false peak of random count arrays as a function of the pollution degree with Gaussian and uniform noise for different rank vector lengths and convolution sizes is demonstrated in Figs. 2–5. Therefore, Figs. 2–5 demonstrate graphs of the true/false peak ratio under different grades of Gaussian noise pollution and lengths of the rank vector of arrays of sinusoidal counts for various preparation methods. Software modelling of suggested preparation methods in processing one-dimensional arrays demonstrate high noise resistance of the method under pollution with the Gaussian noise of up to 20% of the background object.

As Fig. 2 shows, when random count arrays are polluted with uniform noise, the S-preparation method, on average, gives a lower true/false peak ratio as compared to the method of contour preparation. Fig. 3 shows that when the sinusoidal count array is polluted with uniform noise, the method of S-preparation with correction produces a higher true/false peak ratio as compared to the method of contour preparation with the rank vector length $r=1$ and mild noise pollution in the range of 1–10%.

Fig. 4 demonstrates that when a random count array is polluted with the Gaussian noise, the method of

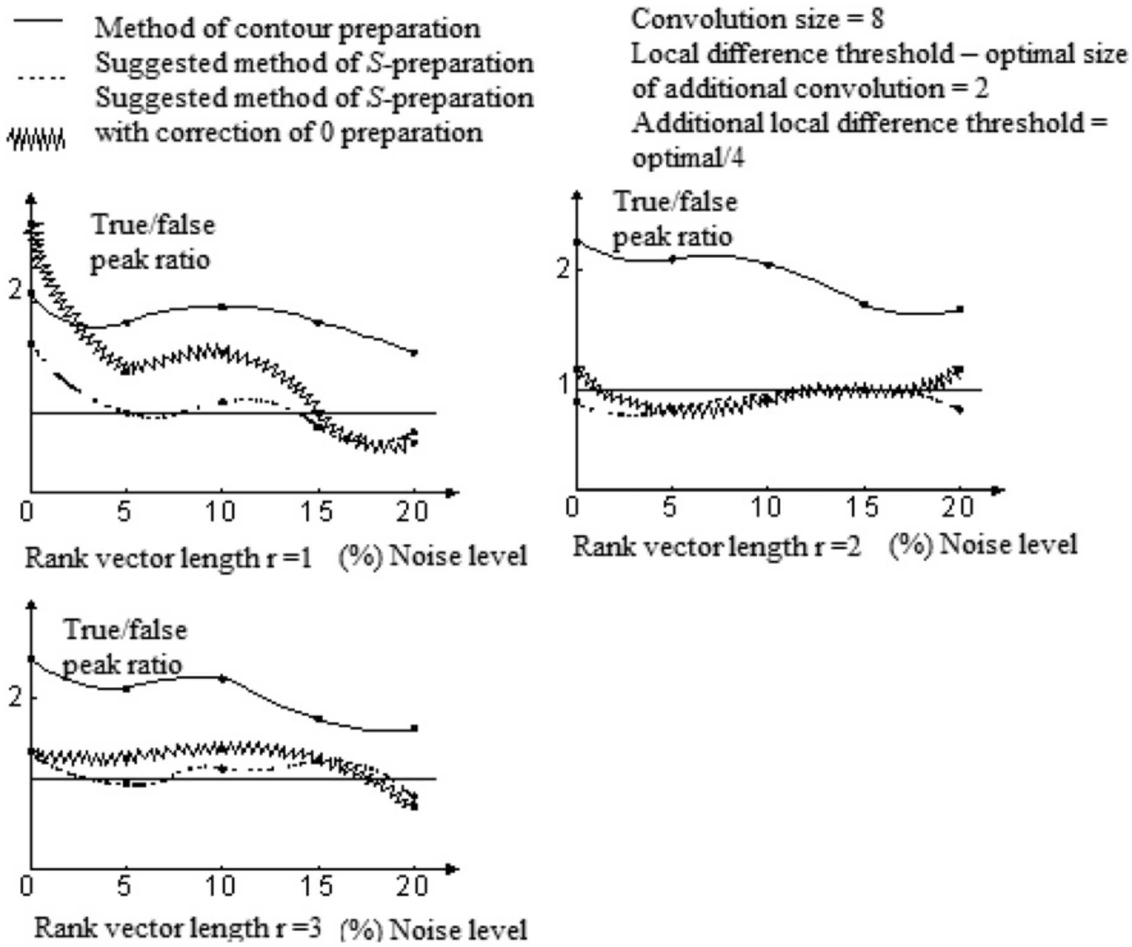


**Fig. 2** *Graphs of the true/false peak ratio under different grades of uniform noise pollution and lengths of the rank vector of arrays of sinusoidal counts for various preparation methods*

S-preparation with correction produces a higher true/false peak ratio in comparison to the method of contour preparation for the rank vector length $r = 1$ and noise pollution in the range of 0–12%.

Fig. 5 demonstrates that when a random count array is polluted with the Gaussian noise, the method of S-preparation with correction produces a higher true/false peak ratio as compared to the method of contour preparation with the noise pollution of 10–20%.

Simulation results may serve for selecting a preparation method, depending on the background characteristics and the level of noise pollution.

To conduct electronic modelling of the synthesised method, a special device was suggested and realised. Its scheme is shown in Fig. 6, where 1 is a video sensor; 2 – ADC; 3 – fragment selection unit; 4 – calculation unit of the local difference threshold; 5 – coder unit; 6 – reference selection unit; 7 – correlator unit; 8 – result calculation unit.

The following main technical parameters of the model device were received as testing results:

Image size: 512 × 512 counts.
Capacity of the video signal digital readout: 6 digits
Image frame frequency: 50 Hz
Selected fragment size: 128 × 128 counts
Background shift measurement range: +/−15 counts
Background shift measurement error: +/−1 count
Pace of the background shift measurement: 20 ms.

Software for modelling the S-preparation method makes it possible to model one-dimensional arrays, model one-dimensional signals, conduct noise processing corresponding to noise distortions of the signal, to distort a scale of one-dimensional arrays, to model the S-preparation method under various initial signals and parameters of S-preparation.

The modelling software has a modular construction and consists of:

- mode selection unit (menu);
- array formation unit;
- array 'insert' unit;
- rescaling unit;
- array noise pollution unit;
- graphing unit;
- fragmentation unit;
- correlation unit.

The correlation unit presents the following options:

- input of two input arrays from a disc;
- set true background shift;
- set noise pollution degree of input arrays;
- set the convolution size;
- set the range of summing window shifts;
- set the rank vector length;
- set a local difference threshold and calculate its optimal value in the process of operation (optional);



doi: 10.1049/iet-ipr.2013.0471

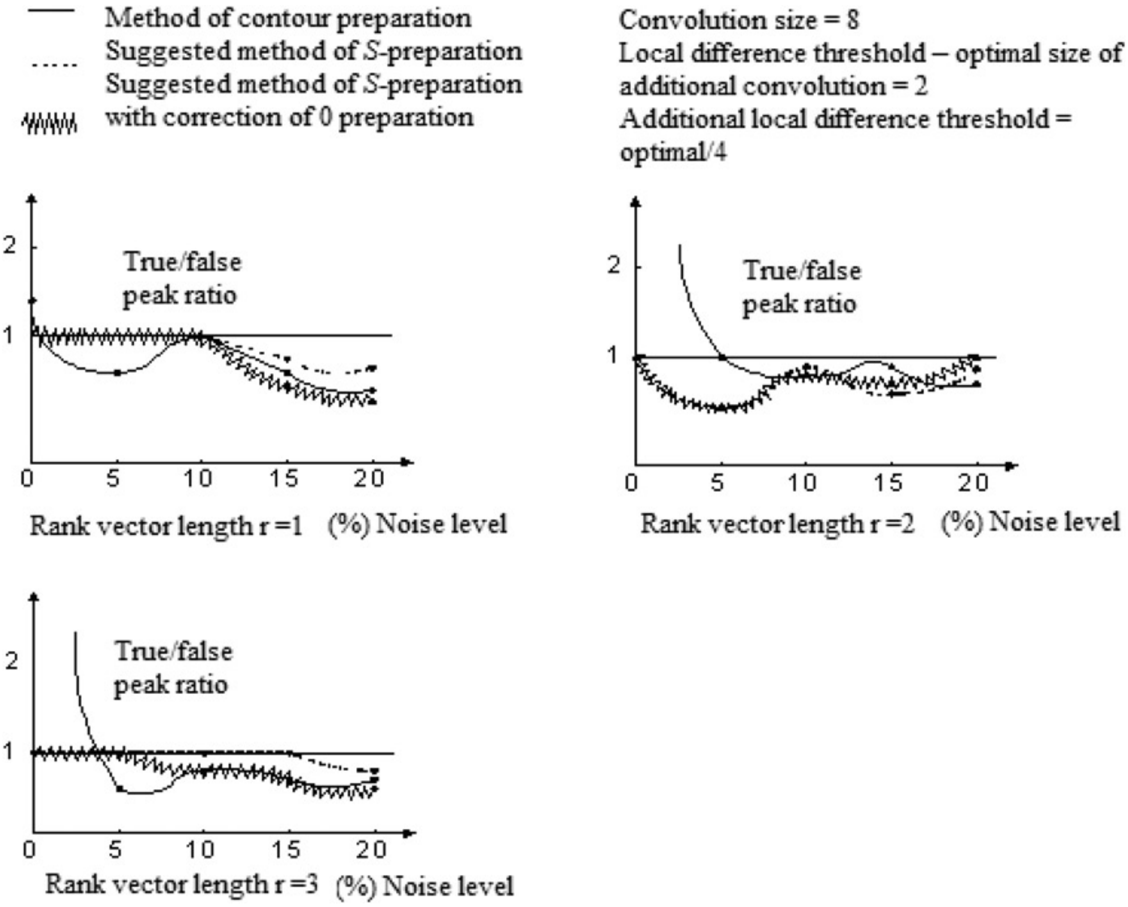


**Fig. 3** *Graphs of the true/false peak ratio under different grades of uniform noise pollution and lengths of the rank vector of arrays of sinusoidal counts for various preparation methods*

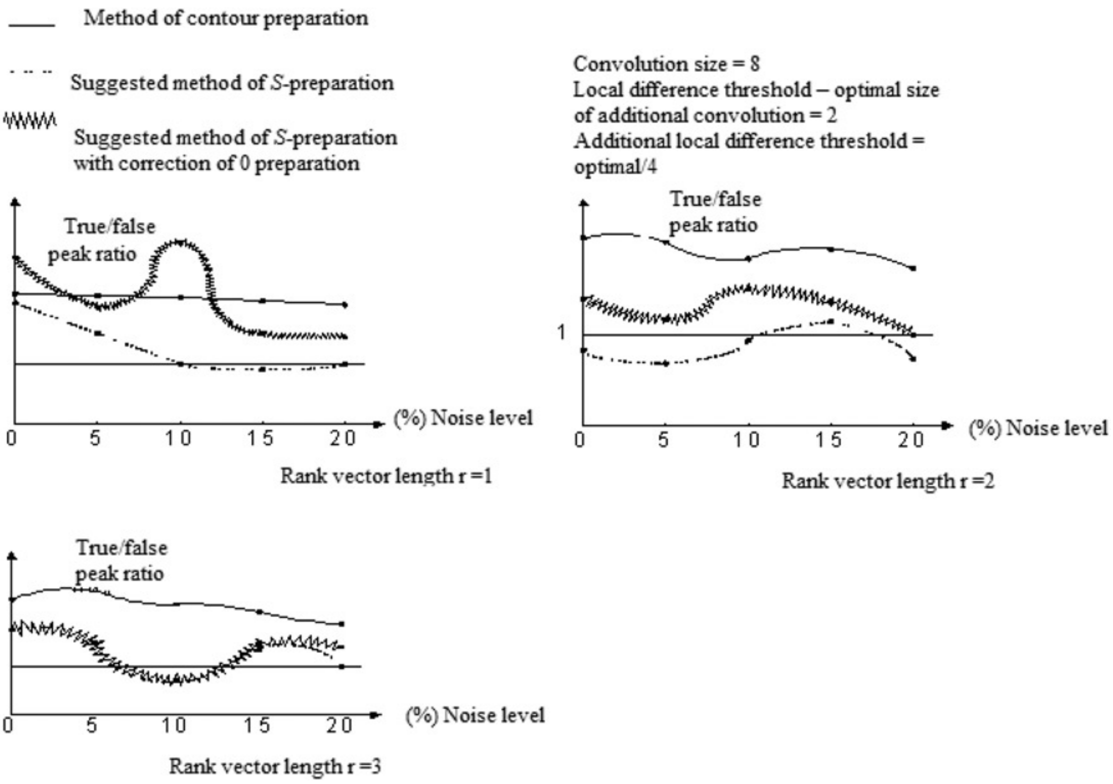


**Fig. 4** *Graphs of the true/false peak ratio under different grades of Gaussian noise pollution and lengths of the rank vector of arrays of random counts for various preparation methods*


doi: 10.1049/iet-ipr.2013.0471

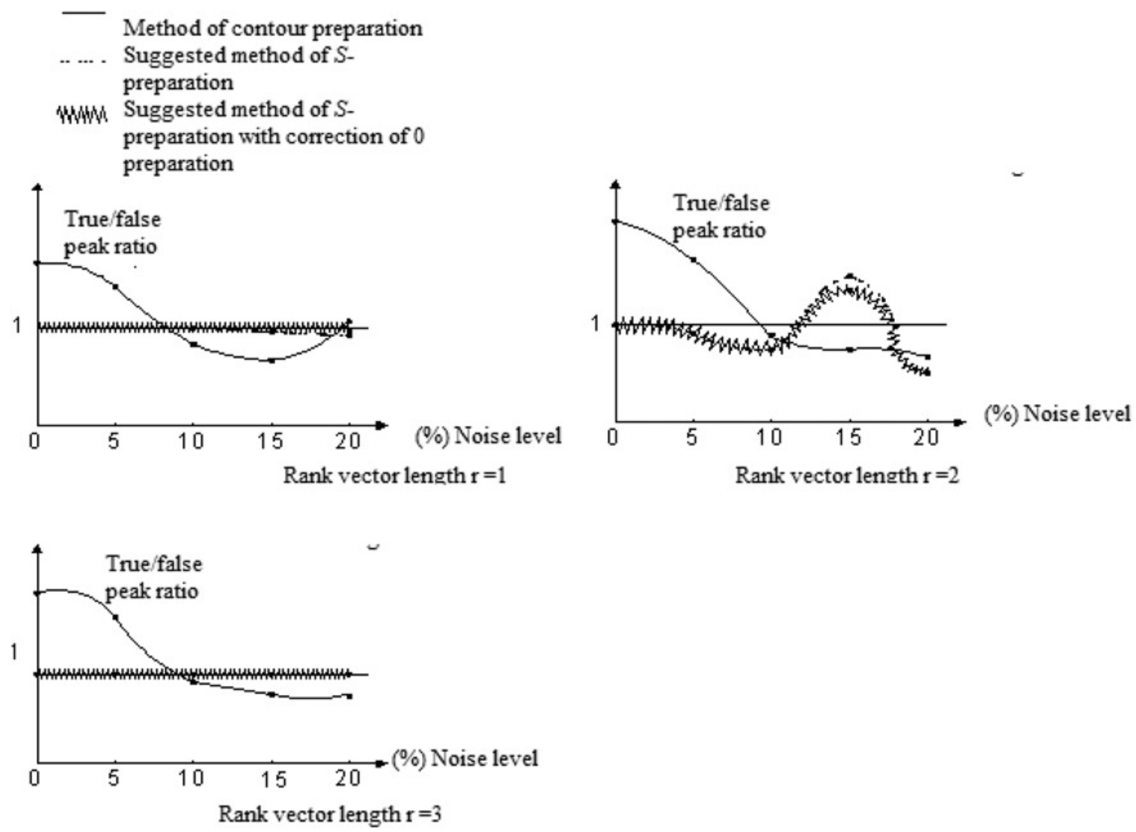


**Fig. 5** *Graphs of the true/false peak ratio under different grades of Gaussian noise pollution and lengths of the rank vector of arrays of sinusoidal counts for various preparation methods*

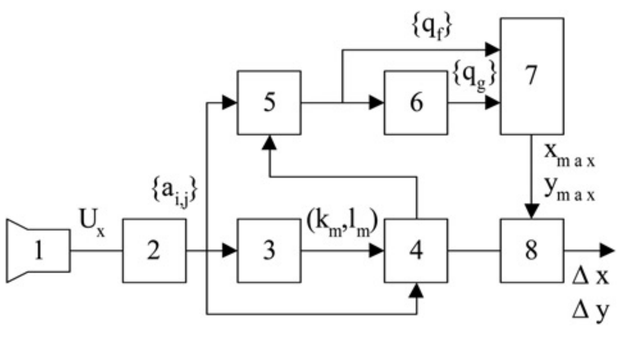


**Fig. 6** *Block chart of the analysis of an extended object localisation*

- correct zero labels;
- set parameters of zero label correction.

The following values are produced as a result of unit operation:

- output array of maximums of label matching of input arrays in the range of summing window shifts;
- a false peak value and a ratio of true/false peak;
- an extremum of label matching maximums and of the respective background shift.

In the process of software modelling, formation of the significant number of zero contour labels, which provide main contribution to formation of the count of the RCCF, was registered for some types of backgrounds (for instance, periodical ones – sinusoidal, saw-toothed); as a result, a ratio of true and false peaks values of the RCCF decreases.

A method of S-preparation may be modified by correcting zero labels, when each image fragment that corresponds to the zero label, is corrected in the following way:

- A selected image fragment is additionally split into smaller fragments, and an addition convolution – an averaged sum of counts falling into the additional fragment – is calculated by the number of counts;
- For each additional fragment, a difference is determined between the values of the additional and main convolutions;
- An averaged sum of positive difference between values of the additional and main convolutions by a number of such positive differences is determined;
- An additional local difference threshold is determined as the main local difference threshold divided by 4 (factor 4 was determined empirically in the process of modelling various types of backgrounds);
- Averaged sums of positive convolutions of corresponding image fragments separated on the rank vector are taken as rank operands. An additional local difference threshold is taken as a local difference threshold. According to the method of contour preparation, new values of the contour labels are formed, corresponding to the given image fragment: ‘ + ’, ‘–’, ‘0’.

Therefore, after correcting zero labels for current and delayed images, new arrays of contour labels ‘ + ’, ‘–’, ‘0’, ‘ + ’, ‘–’ are formed, which are then processed with the method of contour preparation.



doi: 10.1049/iet-ipr.2013.0471

The conducted software and hardware modelling and the comparative analysis of various methods of correlation processing allowed to develop a method of S-preparation, which consists of forming convolutions of image counts under difference shifts of summing window; forming, on this basis, convolutions of contour labels using an optimal local difference threshold; and comparing the obtained labels of the current image with labels of a delayed image under a zero shift of the summing window. This method allows to find coordinates of the true background shift of the image with the accuracy of up to one pixel under the exceeding of the true peak of the RCCF of the maximal false peak for most types of image backgrounds. Exceptions include some cases of backgrounds with regular structure (e.g. sinusoidal). A method of optimisation of the value of the local difference threshold and its linking to a specific type of the image was developed as well.

Based on the mentioned processing methods, a schematic diagram of the correlation analysis unit was developed, representing a 16-channel parallel structure which includes a system controller, a fragment selection unit, a unit of determination of the optimal local difference threshold and a 16-channel convolution and preparation unit. The functional schemes of the unit select a fragment of $128 \times 128$ pixels from the image of $512 \times 512$ and a channel of preparation convolution were developed, too. An analysis of dynamic parameters showed that a full time comparison of contour labels of the current and delayed images of $128 \times 128$ pixels does not exceed 4 ms. Therefore, during one frame (20 ms), processing by two rank vectors is possible.

Authors give this simulation as an illustration in order to assess efficiency of the S-preparation method in detecting a shift for an irregular background and a background with periodic (sinusoidal) regularity, as compared to its known analogue – the method of contour preparation.

Two types of backgrounds were used due to a possibility of the preliminary theoretical assessment of the true/false peak ratio to control simulation results.

Of course, those two types of backgrounds and two types of noise do not reflect a real signal clutter situation. For this reason, the authors think that a comparative modelling of the method of S-preparation with known methods of preprocessing and assessing a background shift with respect to the variety of real and synthesised backgrounds and noises, as well as getting well-grounded theoretical assessments, is an important independent task, which will be dealt by the authors in the nearest future.

## 4 Conclusions

The conducted software and hardware modelling and the comparative analysis of various methods of correlation processing allowed to develop a method of S-preparation, which consists of forming convolutions of image counts under difference shifts of summing window; forming, on this basis, convolutions of the contour labels using an optimal local difference threshold; and comparison of the obtained preparation of the current image with preparations of delayed image under a zero shift of the summing window. This method allows to determine the coordinates of the true shift of the image background, with the accuracy of up to one pixel under exceeding of the true peak of the RCCF of the maximal false peak for most types of image backgrounds. Exceptions include some cases of backgrounds of regular structure (e.g. sinusoidal). A method of local difference threshold optimisation and its linking to a specific type of the image was developed as well.

Based on the abovementioned processing methods, a schematic diagram of a correlation analysis unit was developed, representing a 16-channel parallel structure, which includes a system controller, a fragment selection unit, a unit of determination of the optimal local difference threshold and a 16-channel convolution and preparation unit. An analysis of dynamic parameters showed that a full time comparing of contour labels of the current and delayed images of $128 \times 128$ pixels does not exceed 4 ms. Therefore, during one frame (20 ms), processing by two rank vectors is possible.

## 5 References


1 Ima, J., Jensen, J.R., Tullis, J.A.: 'Object-based change detection using correlation image analysis and image segmentation', *Int. J. Remote Sens.*, 2008, **29**, (2), pp. 399–423

2 Kozhemyako, V.P., Kutaev, Y.F., Timchenko, L.I., *et al.*: 'The *Q*-transformation method applying to the facial images normalization'. Proc. Int. ICSC IFAC Symp. on Neural Computation', Vienna, September 1998, pp. 287–291

3 Perveen, S., James, L.A.: 'Changes in correlation coefficients with spatial scale and implications for water resources and vulnerability data', *The Professional Geogr.*, 2012, **64**, (X), pp. 1–12

4 Spüler, M., Rosenstiel, W., Bogdan, M.: 'One class SVM and canonical correlation analysis increase performance in a c-VEP based brain–computer interface (BCI)'. Proc. 20th European Symp. on Artificial Neural Networks, Bruges, Belgium, April 2012, pp. 103–108

5 Yarovyy, A., Timchenko, L., Kokriatskaia, N.: 'Theoretical aspects of parallel-hierarchical multi-level transformation of digital signals'. Proc. 11th Int. Conf. Development and Application Systems, Suceava, Romania (Suceava, Universitatea Stefan cel Mare Suceava), May 2012, pp. 1–9

6 Sharin, A., Khan, M.R., Imtiaz, H., Sarwar, M.S.U., Fattah, S.A.: 'An efficient face recognition algorithm based on frequency domain cross-correlation function'. Int. Conf. Electrical and Computer Engineering (ICECE), Dhaka, Bangladesh, December 2010, pp. 183–186

7 Zhao, Q., Rutkowski, T.M., Zhang, L., Cichocki, A.: 'Generalized optimal spatial filtering using a kernel approach with application to EEG classification', *Cognit. Neurodyn.*, 2010, **4**, (4), pp. 355–358

8 Pannekoucke, O., Berre, L., Desroziers, G.: 'Background error correlation length-scale estimates and their sampling statistics', *Q. J. R. Meteorol. Soc.*, 2008, **134**, (497–508), pp. 497–511

9 Donev, A., Torquato, S., Stillinger, F.H.: 'Pair correlation function characteristics of nearly jammed disordered and ordered hard-sphere packings', *Phys. Rev. E 71*, 2005, **011105**, pp. 1–14

10 Zhou, Z., Tang, X.: 'New families of binary low correlation zone sequences based on interleaved quadratic form sequences', *IEICE Trans. Fundam. Electron. Commun. Comput. Sci.*, 2008, **E91-A**, (11), pp. 3406–3409

11 Zou, K.H., Hall, W.J.: 'On estimating a transformation correlation coefficient', *J. Appl. Stat.*, 2002, **29**, (5), pp. 745–760

12 Awwal, A.A.S., Rice, K.L., Taha, T.M.: 'Fast implementation of matched-filter-based automatic alignment image processing', *Opt. Laser Technol.*, 2009, **41**, (2), pp. 193–197

13 Cherkasov, A., Sprous, D.G., Chen, R.: 'Three-dimensional correlation analysis. a novel approach to the quantification of substituent effects', *J. Phys. Chem. A*, 2003, **107**, (45), pp. 9695–9704

14 Peña-Ortega, C., Vélez-Reyes, M.: 'Evaluation of different structural models for target detection in hyperspectral imagery'. Proc. SPIE Orlando, Florida, 2010, vol. 7695, pp. 76952H–76952H-11

15 Shawakfen, O.Q., Gertsiy, A.A., Timchenko, L.I., Kutaev, Y.F., Zlepko, S.M., Shveyki, N.: 'Method of recursive-contour preparing for image normalization'. Proc. IEEE-EURASIP Workshop on Nonlinear Signal and Image Processing, Antalya, Turkey, 1999, pp. 414–418

16 Thirumalai, V., Frossard, P.: 'Distributed representation of geometrically correlated images with compressed linear measurements', *IEEE Trans. Image Process.*, 2012, **21**, (7), pp. 3206–3219

17 Kou, G., Lu, Y., Peng, Y., Shi, Y.: 'Evaluation of classification algorithms using MCDM and rank correlation', *Int. J. Inf. Technol. Decis. Mak. (IJITDM)*, 2012, **11**, (01), pp. 197–225

18 Zhao, J., Zhang, J., Yin, J.: 'A parallel differential correlation acquisition algorithm in time domain'. Fifth Int. Conf. Wireless Communications,



doi: 10.1049/iet-ipr.2013.0471

Networking and Mobile Computing, 2009. WiCom '09, Shanghai, China, September 2009, pp. 1–4

19 Argyriou, V.: 'Sub-hexagonal phase correlation for motion estimation', *IEEE Trans. Image Process.*, 2011, **20**, (1), pp. 110–120

20 Kozhemyako, V., Timchenko, L., Yarovyy, A.: 'Methodological principles of pyramidal and parallel-hierarchical image processing on the base of neural-like network systems', *Adv. Electr. Comput. Eng.*, 2008, **8**, (2), pp. 54–56

21 Timchenko, L.I., Kutaev, Y.F., Chepornyuk, S.V., Grudin, M.A., Harvey, D.M., Gertsiy, A.A.: 'A brain-like approach to multistage hierarchical image'. Proc. Image Analysis and Processing, Italy, 1997, pp. 246–253



doi: 10.1049/iet-ipr.2013.0471